Journal of Soils and Sediments (2021) 21:1644–1658
https://doi.org/10.1007/s11368-021-02910-5

SOILS, SEC 1 • SOIL ORGANIC MATTER DYNAMICS AND NUTRIENT CYCLING • RESEARCH ARTICLE

Changes in soil carbon and nitrogen accessibility with the application of biochars with different morphological and physical characteristics

Michaela Sedláková[1] · Jiřina Száková[1] · Miloslav Lhotka[2] · Niguss Solomon Hailegnaw[1] · Zlata Holečková[1] · Kateřina Pračke[1] · Tatiana Robledo-Mahón[1] · Pavel Tlustoš[1]

Received: 10 June 2020 / Accepted: 18 February 2021 / Published online: 24 February 2021

Abstract

Purpose The recent literature indicates that, depending on the feedstocks and pyrolysis temperature, biochar can be a good source of nutrients. On the contrary, some biochars are not good sources of available carbon and other nutrients, but their porous structure seems to be a suitable microenvironment for microbial colonization. We investigated the response of soil biological parameters, microbial biomass carbon and nitrogen (MBC and MBN), in relation to mobile N species.

Material and methods Five different biochars were produced at different temperatures (300, 350, 400, 450, and 500 °C) from the same feedstock (woodchips). The physicochemical and morphological characteristics of the individual biochar samples were described, and incubation was carried out with the application of 2% biochar to two different soil types (luvisol and fluvisol).

Results and discussion The addition of 2% biochar did not change the pH in the slightly acid soils used in the experiment, in spite of the alkaline character of biochar. The increasing amounts of total and nitrate-available nitrogen during the experiment are probably related to changes in soil microbial activity. The amount of soluble carbon was constant during the experiment, confirming its stability in the soil, most likely because of the high amount of lignin in the feedstock. The influence of biochar on the soil microbiome was determined on the basis of the concentrations of MBC and MBN. Microbial biomass was increased in both soils treated with biochar produced at lower temperatures.

Conclusions The physicochemical characteristics of the biochar as well as the sorption behavior of N-NO_3^- and N-NH_4^+ indicate that at a pyrolysis temperature of 400 °C, biochar properties change substantially. However, these findings are only valid for biochar produced from woodchips, and the long-term effects of biochar application on soil properties need to be investigated in further studies.

Keywords Biochar · Soil amendment · Microbial biomass · Nitrogen

1 Introduction

Biochar is a carbon-rich material, the result of the thermochemical decomposition of organic matter in the absence of oxygen. The production of biochar is analogous to the traditional production of charcoal, but the term "biochar" is related to the material being intended for soil applications (Lehmann and Joseph 2009). Biochars are one of the most intensively and extensively investigated soil additives in terms of their production, application, and fate in the soil due to their benefits such as increasing soil quality and fertility (Zhang et al. 2018). The detailed technological aspects as well as the characteristics of the individual products were already reviewed for instance by Novotny et al. (2015), Kan et al. (2016), and Tripathi et al. (2016). The pyrolysis temperature in the

Responsible editor: Zucong Cai

✉ Jiřina Száková
szakova@af.czu.cz

[1] Department of Agro-Environmental Chemistry and Plant Nutrition, Faculty of Agrobiology, Food and Natural Resources, Czech University of Life Sciences, Kamýcká 129, Prague 6-, Suchdol, Czech Republic

[2] Department of Inorganic Technology, Faculty of Chemical Technology, University of Chemistry and Technology, Prague, Technická 5, 166 28 Prague 6, Czech Republic

reviewed studies varied from 100 to 1000 °C, with a heating rate ranging from 3 to 20 °C min^{-1}. However, the mild pyrolysis of biomass at the temperatures between 200 and 300 °C is the so-called torrefaction, where the devolatilization and carbonization rates depend on the biomass composition (Bates and Ghoniem 2012; Bergman and Kiel 2005). At temperatures less than 200 °C, predominant moisture loss was recorded by the thermogravimetric analysis regardless of the biomass type (Břendová et al. 2017). Thus, the high variability of the feedstocks led to a high variability of the produced biochars, where the total carbon content varied between 40 and 90%. In contrast, the final carbon content and the presence of other elements mostly depend on the origin of the feedstock, the pH level, and other physical characteristics such as specific surface and porosity, which are also strongly affected by the pyrolysis conditions (Zhao et al. 2013).

A biochar is a microporous material, where the porosity increases with the pyrolysis temperature (Dutta et al. 2015). Jimenez-Cordero et al. (2013) found the highest distribution of micropores (0.1–0.4 nm) in a biochar from grape seeds pyrolyzed at 700–800 °C. Generally, the specific surface of a biochar is influenced by the feedstock material and increases with increasing pyrolysis temperature (Chen et al. 2011; Keiluweit et al. 2010; Chen et al. 2008). The molar element ratio is a suitable standard parameter for estimating biochar polarity. Increasing pyrolysis temperature increases the total carbon content, but functional groups such as –OH are released. Thus, biochars prepared at high temperatures are less polar and more stable than those prepared at low temperatures (Novak et al. 2009).

Current knowledge on the behavior of biochars in soil is ambiguous, and the soil–biochar interaction depends on many factors including soil properties, biochar composition, specific surface, porosity, and pyrolysis temperature. The available results suggest that the influences of a biochar on soil physical and chemical properties vary with different application conditions. Biederman and Harpole (2013) subjected globally published findings concerning soil–biochar interactions to detailed statistical tests and found that despite the variability introduced by soil and climate, the addition of a biochar to soils resulted, on average, in improved properties such as aboveground biomass productivity, crop yield, soil microbial biomass, rhizobia nodulation, soil phosphorus, potassium, total nitrogen and carbon, and soil pH increment compared to control conditions.

Since a biochar is a potentially diverse niche for microorganisms, its application to soils may assist in the preservation and support of soil biodiversity, making it a biotope for micro- and mesobiota (Beesley et al. 2011). The porous character of biochars provides an environment for soil microbiota, such as bacteria (0.3–3 μm), fungi (2–80 μm), and protozoans (7–30 μm), and protects them against predators (Zackrisson et al. 1996; Warnock et al. 2007). Thus, the diameter of the biochar pores is important for the colonization of the biochar by microbiota communities. Sasidharan et al. (2016) described the influence of biochar particle size on soil bacteria retention ability in a laboratory column experiment. The addition of a biochar (10% w/w) to sand enhanced the retention of bacteria. However, elimination of the fine fraction of biochar particles (< 60 μm) significantly reduced bacterial retention. Therefore, the authors suggested that the alteration of biochar pore and particle size may play a major role for the soil microbiome.

Additional chemical characteristics of a biochar which influence its microbial colonization are (i) surface charge, which enables the retention of microorganisms, ions, and/or other substances; (ii) the available nutrients and dissolved organic carbon released from the biochar matrix (Gul et al. 2015; Lehmann et al. 2011). The chemical stability of a biochar does not allow microorganisms to use the biochar carbon directly, but the carbon can be gradually leached and mineralized (Lehmann et al. 2011). Gul et al. (2015) reported a positive effect of a biochar prepared at temperatures not exceeding 500 °C from non-wood biomass on the soil microbiome. In contrast, biochars pyrolyzed at higher temperatures (700 °C) did not cause any shifts in microbial communities (Imaparato et al. 2016). Similar results were also reported by Ahmad et al. (2016), who observed an increased abundance of gram-positive and gram-negative bacteria as well as fungi, actinomycetes, and arbuscular mycorrhizal fungi in soils treated with a biochar produced at 300 °C, but not in soils treated with biochars prepared at 700 °C. This might have been caused by the existence of fixed or non-labile carbon in biochars prepared at certain temperatures.

Nutrient leachability also depends on the biochar composition, affected by the feedstock (Zhang et al. 2015). The biochar alters the nutrient balance in the soil and can therefore be considered a source of nutrients such as Ca, P, and K. In contrast, the nitrogen content and availability in biochar-treated soil are questionable due to the heterocyclization of N during pyrolysis (Zheng et al. 2013). Hailegnaw et al. (2019a) also reported poor estimation of ammonium adsorption by biochar due to the liberation of ammonia. In this context, this study investigates the potential changes of nitrogen and carbon mobility in biochar-treated soils as affected by increasing pyrolysis temperature and, therefore, as affected by changing morphological and physicochemical characteristics of the biochar.

The reviewed literature indicates that biochar is, in comparison with soil, not a good source of available carbon and other nutrients, but its porous structure seems to be a suitable microenvironment for microbial colonization, and the different characteristics of micro- and macropores in the individual biochars differently influence the diverse groups of organisms. For instance, Ahmad et al. (2016) found that the changes in bacterial communities in biochar-treated soils strongly

depended on the feedstock type and pyrolysis temperature, which affected the physicochemical properties of the biochar. However, these aspects have not yet been fully elucidated and need further investigation. This study presents the fate of the microbiome, estimated as microbial biomass carbon and nitrogen, in soils treated with woodchip-based biochars produced at different pyrolysis temperatures. In this context, the short-term experiment was established to assess the immediate response of the soil microbiome on the biochar application. While Hailegnaw et al. (2019a) evaluated in detail the response of mobile forms of soil nitrogen as affected by soil type and biochar rate, this study highlights the role of the biochar composition as affected by the pyrolysis temperature. For this purpose, two soils differing in their sorption characteristics (clay content and cation exchange capacity) were chosen for the experiment, to estimate the potential role of soil sorption characteristics in the response of soil biological parameters on the biochar application.

2 Material and methods

2.1 Biochar production and experimental design

For the biochar preparation, commercially available woodchips from spruce and fir wood (CAT'S BEST Universal, Germany SRN) were used. Pyrolysis was performed with the pyrolytic furnace Carbolite 301 (Carbolite Gero, Great Britain) in an electrically heated quartz tube for 25 min at the target temperatures of 300, 350, 400, 450, and 500 °C in the presence of nitrogen (nitrogen flow 4.5 L per min). The feedstock input for one pyrolysis run was 300 g. The biochar was homogenized, and the contents of nutrients and risk elements were determined prior to the experiment.

Two soils differing in their physicochemical parameters, especially in their clay content and cation exchange capacity (CEC), were chosen for the incubation experiment: (i) luvisol from the location Hněvčeves (East Bohemia, Czech Republic); GPS 50° 18′ 46″ N, 15° 43′ 3″ E, pH 5.8, CEC 116 mmol/kg, clay content 26.4%, oxidizable carbon content (C_{ox}) 0.93%, total nitrogen content 0.17%; (ii) fluvisol from the location Choťánky (Central Bohemia, Czech Republic); GPS 50° 8′ 47″ N, 15° 10′ 4″ E, pH 6.4, CEC 55.6 mmol/kg, clay content 12.5%, C_{ox} 3.4%, total nitrogen content 0.14%. The soil samples were taken from arable land in the 0–25-cm layer, dried in the laboratory at ambient temperature, homogenized, and sieved through a 2-mm-diameter mesh.

For the incubation experiment, 245 g of soil + 5 g of biochar were thoroughly mixed in polypropylene bottles to achieve a biochar application rate of 2% (w/w). Control samples containing 250 g of soil were included. Each treatment was established in triplicate, and the soils were watered up to 60% of maximum water-holding capacity. The samples were incubated for 1, 7, 14, 21, and 28 days; at these dates, the samples were split into two parts, of which one was immediately used for determination of biological and chemical soil characteristics and the other one was dried at 105 °C for determination of dry mass content. This parameter was used for recalculation of the determined values to dry soil mass.

2.2 Analytical methods

2.2.1 Biochar characterization

The morphology of the biochar was evaluated by scanning electron microscopy (SEM), using a Hitachi S-450 with an EDS analyzer Kevex Delta 5. Analysis of the infrared spectra was provided by using Fourier transform infrared spectroscopy (FTIR), where a Nicolet 6700 FTIR spectrometer (Thermo Scientific) was coupled with a GladiATR measurement cell (PIKE) and a DTGS detector. The spectra were measured in a spectral range of 400–4000 cm^{-1}, with a resolution of 4 cm^{-1} and with 64 spectra accumulations. The spectra were evaluated by using the Omnic 8.3 (Thermo Scientific) program, as in previous investigations by Melo et al. (2013) and Rafiq et al. (2016).

Specific surface area, micropore analysis, and distributions of volume mesopores were measured on an ASAP 2020 (accelerated surface area and porosimetry) analyzer (Micromeritics, Norcross, GA, USA) using the gas sorption technique (Brewer et al. 2014). The adsorption isotherms of N_2 were fitted by using the Brunauer–Emmett–Teller (BET) method for specific surface area (Brunauer et al. 1938), the micropore volume by the t-plot method (Webb and Orr 1997), and the pore size distribution by the Barrett–Joyner–Halenda (BJH) method (Barrett et al. 1951). Mercury porosimetry measurements were made using an AutoPore IV 9500 porosimeter (Micromeritics, Norcross, GA, USA). A more detailed description of the applied methods was presented by Břendová et al. (2017).

2.2.2 Total element contents of biochars and physicochemical parameters of soils

The pH values of the original soils and the biochar-treated soils were determined in 0.01 mol L^{-1} $CaCl_2$ extract (1:10 w/v). For determination of element content in the biochars, an aliquot (~ 500 mg of dry matter) of the biochar was weighed in a digestion vessel. Concentrated nitric acid (8.0 mL) (Analytika Ltd., Czech Republic) and 30% H_2O_2 (2.0 mL) (Analytika Ltd., Czech Republic) were added, and the mixture was heated in an Ethos 1 (MLS GmbH, Germany) microwave-assisted wet digestion system for 30 min at 220 °C. After cooling, the digests were transferred into a 25-mL glass tube, topped up with deionized water, and kept at

laboratory temperature until measurements were taken (Tůmová et al. 2020).

Inductively coupled plasma-atomic emission spectrometry (ICP-OES), using an Agilent 720 (Agilent Technologies Inc., USA) equipped with a two-channel peristaltic pump, a Struman-Masters spray chamber, and a V-groove pneumatic nebulizer made of inert material, was used to determine the Al, As, B, Cd, Cr, Cu, Fe, Mn, Na, Ni, Pb, Zn, P, and S concentrations of the biochar digests (spectrometry parameters were power, 1.2 kW; plasma flow, 15.0 L min^{-1}; auxiliary flow, 0.75 L min^{-1}; nebulizer flow, 0.9 L min^{-1}). Flame atomic absorption spectrometry, using a Varian 280FS (F-AAS, Varian, Australia), was used to determine the Ca, Mg, and K contents of the solutions. For the determination of total carbon and nitrogen in biochars, a CHNS Vario MACRO cube (Elementar Analysensysteme GmbH, Germany) analyzer was used. About 25 mg of the sample was burned in a catalytic furnace, and subsequently, C and N were determined using a thermal conductivity detector. Inorganic N forms ($N\text{-}NH_4^+$ and $N\text{-}NO_3^-$) and dissolved organic matter (DOC) were determined via a SKALAR San Plus System continuous flow-segmented analyzer (Skalar, Netherlands).

2.2.3 Batch sorption experiment

The batch sorption experiment was conducted with the use of concentrated NH_4NO_3 and subsequent dilution to obtain concentrations of $N\text{-}NO_3^-$ and $N\text{-}NH_4^+$ in the range between 10 and 1000 mg L^{-1}. Subsequently, 30 mL of the NH_4NO_3 solution and 0.1 g of biochars were shaken for 24 h at 120 rpm in a horizontal shaker to obtain an equilibrium state, and only NH_4NO_3 solution was included as control. The biochar NH_4NO_3 mixture and the NH_4NO_3 solution were agitated for 24 h, and the supernatant was filtered through a filter paper. The amount of $N\text{-}NO_3^-$ and $N\text{-}NH_4^+$ was measured by the fluorometric method, using a microplate reader (Infinite M200, Tecan France SAS, France) operated at 30 °C and controlled by the i-control™ software (Robert-Peillard et al. 2017; Ciulu et al. 2018). After the measurement, the amounts of $N\text{-}NO_3^-$ and $N\text{-}NH_4^+$ adsorbed by biochars were determined via Eq. 1:

$$Q_e = (C_0 - C_e)\, V/M \tag{1}$$

where Q is the amount of $N\text{-}NO_3^-$ or $N\text{-}NH_4^+$ adsorbed by biochar (mg g^{-1}), C_0 is the amount of $N\text{-}NO_3^-$ or $N\text{-}NH_4^+$ in the original/control solution (mg L^{-1}), C_e is the concentration of $N\text{-}NO_3^-$ or $N\text{-}NH_4^+$ at the equilibrium state with biochar (mg L^{-1}), V is the volume of NH_4NO_3 solution used (L), and M is the mass of the used biochar (g). After the quantification of sorbed $N\text{-}NO_3^-$ and $N\text{-}NH_4^+$, they were fitted to Freundlich and Langmuir isotherms, as presented in Eqs. 2 and 3, respectively (Limousin et al. 2007):

$$Q_F = FC^n \tag{2}$$

where Q_F is the amount of adsorbed $N\text{-}NO_3^-$ or $N\text{-}NH_4^+$ by biochar (mg g^{-1}), F is the Freundlich isotherm constant (mg g^{-1}), C is the equilibrium concentration of $N\text{-}NO_3^-$ or $N\text{-}NH_4^+$, and n is the adsorption intensity (mg L^{-1}).

$$Q_L = Q_{max}\,[LC/(1+LC)] \tag{3}$$

where Q_L is the amount of sorbed $N\text{-}NO_3^-$ or $N\text{-}NH_4^+$ by biochar (mg g^{-1}), Q_{max} is the maximum sorption capacity of biochar (mg g^{-1}), L is the Langmuir isotherm constant, and C is the equilibrium concentration of $N\text{-}NO_3^-$ or $N\text{-}NH_4^+$ (mg L^{-1}). The isotherms of Freundlich and Langmuir were fitted using Sigma plot for Windows version 11.0.

2.2.4 Soil biological parameters

Microbial biomass carbon (MBC) and nitrogen (MBN) in soil samples were determined by the chloroform fumigation/extraction method modified by Gregorich et al. (1990). Briefly, 10 g of soil sample was placed into a vacuum desiccator and subjected to chloroform vapors for 24 h. After that, the total organic carbon (TOC) was extracted using 0.5 M K_2SO_4 in a ratio of 1:4 (w/v), shaken for 60 min, and determined using the dichromate oxidation method (Mingorance et al. 2007; García-Sánchez et al. 2016). Inorganic N forms ($N\text{-}NH_4^+$ and $N\text{-}NO_3^-$) and dissolved organic matter (DOC) were determined via the abovementioned SKALAR San Plus System continuous flow-segmented analyzer (Skalar, Netherlands). The MBC was calculated as C = EC/kEC, where EC = (organic C extracted from fumigated soils) − (organic C extracted from non − fumigated soils) and kEC = 0.45 (Wu et al. 1990). The MBN was calculated as N = EN/kEN, where EN = (total N extracted from fumigated soils) − (total N extracted from non − fumigated soils) and kEN = 0.54 (Brookes et al. 1985).

2.3 Data analysis

The statistical analyses were performed using the Statistica 12.0 software (StatSoft, Tulsa, USA). One-way analysis of variance (ANOVA) at $p < 0.05$, followed by Tukey's test, was applied to assess the effects of the individual treatments. The interactions of the treatment and other variables (e.g., pyrolysis temperature, soil) were analyzed by factorial analysis of variance, ANOVA, where the significance was assessed at $p < 0.05$, $p < 0.01$, and $p < 0.001$. Correlation analysis was

used for the assessment of relationships between variables, where Pearson's correlation was used with $p < 0.05$ as the criterion for significance.

3 Results and discussion

3.1 Biochar characteristics

The different pyrolysis temperatures applied in this experiment resulted in different biochar yields from similar feedstocks; yield decreased from 34% at 300 °C to 21% at 500 °C. Pyrolysis of biomass results in the decomposition of cellulose, hemicellulose, and lignin and, simultaneously, in the release of volatile compounds (Wu et al. 2012; Zhao et al. 2013; Zhang et al. 2015). Figure S1 shows the average FTIR responses of the individual biochar samples. A decreasing abundance of –OH groups with increasing pyrolysis temperatures (wavenumbers around 3350 cm^{-1}) was observed, with a similar trend for aliphatic C-H vibrations (wavenumbers between 2800 and 3000 cm^{-1}); we also observed bending vibrations of the C-H bonds (wavenumbers between 1400 and 1450 cm^{-1}). The abundance of spectral bands of these vibrations at pyrolysis temperatures higher than 400 °C was almost negligible.

The spectral bands around wavenumbers 1600 cm^{-1} are related to aromatic C=C vibrations partially overlapped by the carbonyl C=O vibrations of organic matter (wavenumbers around 1695 cm^{-1}). This band gradually decreased with increasing pyrolysis temperatures, as observed for the aliphatic groups. The bands apparent at wavenumbers between 750 and 900 cm^{-1} represent aromatic C-H bonds. The presence of spectral bands at wavenumbers 1055 cm^{-1} (related to aliphatic C-O-C vibrations) and 1160 cm^{-1} (related to –OH groups) indicates residues of cellulose and hemicellulose in the biochars pyrolyzed at 300–350°C. At higher pyrolysis temperatures, these bands disappeared. Biochar properties are affected not only by the pyrolysis temperature but also by the feedstock (Lu et al. 2009). The pyrolysis of lignin-containing feedstocks, such as wood biomass, results in a higher abundance of more stable aromatic compounds compared to those containing more cellulose and hemicellulose (Azargohar et al. 2013, 2014; Nanda et al. 2014; Mohanty et al. 2013; Stefanidis et al. 2014; Brown et al. 2011), as indicated also by this study.

The decrease in biochar yield is accompanied by a stepwise increment in the percentage of carbon and the contents of most of the macronutrients and micronutrients in the biochar with increasing pyrolysis temperatures (Table 1) due to carbonization and ashing processes, as observed also by Nanda et al. (2016). In the case of N and S, their contents remained stable for temperatures higher than 350 °C. Therefore, partial loss of these elements via volatilization at the higher pyrolysis temperatures cannot be excluded. Similarly, Cd seemed to be volatilized because its contents in the biochars decreased with increasing pyrolysis temperatures. The contents of other risk elements, As and Pb, were below the detection limit of the ICP-OES technique. Thus, the biochars investigated in this study can serve as a potential source of nutrients without any risk of soil contamination with As, Cd, and Pb.

The differences in the physical structure of the biochars as affected by the pyrolysis temperature are presented in Figs. 1, 2, and 3, and the specific surface areas and pore volumes are summarized in Table 2. All samples of biochars pyrolyzed at low temperatures (up to 350 °C) showed N_2 adsorption isotherms of type II (IUPAC classification, IUPAC 2015), indicating that the samples have a non-porous or macroporous structure, where the specific surface area was less than 1 m^2 g^{-1}. Figure 1 shows the N_2 (77 K) adsorption and desorption isotherms of type Ia (IUPAC classification, IUPAC 2015) for samples of biochars pyrolyzed at higher temperatures (up to 400 °C). These results show a rapid increase in the abundance of small pores, when the pyrolysis temperature increases from 400 to 450 °C, as well as the increase of N_2 adsorption by one order of magnitude from 400 to 450 °C and the similar increase of the specific surface area. The specific surface area (S_{BET}) of biochars was 179.82 m^2 g^{-1} (400 °C) and 385.65 m^2 g^{-1} (450 °C), but the specific surface area ($S_{t\text{-}plot}$) was 18.32 m^2 g^{-1} (400 °C) and 58.94 m^2 g^{-1} (450 °C), indicating an increase in the number of micropores (Table 2).

The abundance of macropores was also apparent from Fig. 2, presenting the results of mercury porosimetry. Figure 3 shows a low abundance of mesopores in all biochar samples, where predominantly very small mesopores and micropores are present, similar to the values of the smallest pores compared to the total pore volume, confirming the predominance of micropores in this case (Table 2). Figures 1, 2, and 3 indicate the possible sintering of the macropores to lower diameters with increasing pyrolysis temperatures. The change in biochar porosity as affected by the pyrolysis temperature is also documented by the SEM images of the morphological structure of the individual biochar samples (Fig. S2). Therefore, based on these results, biochars from woodchips can be separated into two groups with different physicochemical parameters, where the pyrolysis temperature of 400 °C seems to be the delimiting parameters for estimation of the expected biochar characteristics.

3.2 Incubation experiment

3.2.1 Available carbon and nitrogen contents in soil

Biochar is considered a soil amendment similar to the application of lime because of its high contents of alkali and alkaline earth metals, as well as carbonates, resulting in a soil pH increase by up to one unit of measurement (Gaskin et al. 2008;

Table 1 Total contents of selected elements in biochars ($n = 3$)

	300 °C	350 °C	400 °C	450 °C	500 °C
Al (mg/kg)	41.4 ± 0.8	52.6 ± 3.8	67.6 ± 0.4	72.5 ± 5.4	76.0 ± 3.2
B (mg/kg)	6.08 ± 0.63	6.23 ± 1.32	7.23 ± 1.18	8.90 ± 1.18	8.90 ± 0.13
Ca (mg/kg)	2090 ± 14	2752 ± 91	3460 ± 118	3907 ± 348	3843 ± 137
Cd (mg/kg)	0.305 ± 0.008	0.356 ± 0.016	0.158 ± 0.014	0.039 ± 0.003	0.041 ± 0.017
Cr (mg/kg)	0.319 ± 0.012	0.481 ± 0.048	0.491 ± 0.000	0.563 ± 0.122	0.608 ± 0.096
Cu (mg/kg)	1.86 ± 0.29	2.14 ± 0.04	3.11 ± 0.54	3.09 ± 0.21	2.87 ± 0.14
Fe (mg/kg)	35.1 ± 0.0	45.2 ± 10.3	66.5 ± 3.9	63.0 ± 5.6	64.2 ± 10.4
K (mg/kg)	828 ± 4	1171 ± 9	1424 ± 51	1607 ± 104	1635 ± 15
Mg (mg/kg)	351 ± 3	473 ± 14	558 ± 12	649 ± 54	629 ± 13
Mn (mg/kg)	44.8 ± 8.2	104 ± 3.4	152 ± 10.9	135 ± 1.4	181.2 ± 3.5
Na (mg/kg)	24.2 ± 0.6	30.3 ± 0.2	39.8 ± 0.7	44.7 ± 2.5	44.5 ± 0.3
Ni (mg/kg)	0.125 ± 0.008	0.278 ± 0.051	0.274 ± 0.040	0.314 ± 0.080	0.340 ± 0.008
P (mg/kg)	127 ± 3	168 ± 11	203 ± 6	230 ± 17	224 ± 14
S (mg/kg)	50.1 ± 2.6	64.0 ± 0.7	68.6 ± 0.4	68.9 ± 4.9	64.6 ± 0.8
Zn (mg/kg)	18.6 ± 1.0	24.8 ± 1.0	28.8 ± 0.1	33.8 ± 3.7	31.4 ± 2.4
N (%)	0.100 ± 0.010	0.139 ± 0.050	0.140 ± 0.009	0.146 ± 0.002	0.144 ± 0.012
C (%)	68.3 ± 0.1	73.5 ± 0.2	76.0 ± 0.3	79.6 ± 0.3	83.8 ± 0.0

Novak et al. 2009; Sun and Li 2014; Lehmann 2007). However, no unambiguous pH change of biochar-treated soils during the incubation experiment was observed in our study (Fig. 4). In contrast, Gaskin et al. (2008) reported that biochars based on poultry litter or peanut hulls are characterized by pH levels close to 10, and pyrolysis of pine chips resulted in a biochar pH of around 8. Moreover, the contents of the alkali and alkaline earth metals in the biochars based on poultry litter exceed those in the pine chips by one or two orders of magnitude (Gaskin et al. 2008). The element contents in the woodchip biochar used in this experiment (Table 1) were comparable to the elemental composition of the pine chips cited above. Additionally, the mobile proportions of the main macro- and micronutrients in the biochar-treated soils (except Cu and K) decreased during the incubation experiment with increasing pyrolysis temperatures (Sedláková et al. 2019). Zhao et al. (2013) assumed that the pH level of the biochar is predominantly affected by the pyrolysis conditions. For instance, Hailegnaw et al. (2019b) reported a significant increase in pH levels in the soils, with pH ≤ 6.2 after the application of 2% of wood chip biochar pyrolyzed at 700 °C. In this experiment, woodchip biochars produced at low temperatures showed no significant effect on the pH levels of both slightly acidic soils at a 2% rate during the entire incubation experiment, most probably due to both low pyrolysis temperatures and low contents of alkaline elements.

The contents of inorganic N forms (N_{tot}, N-NH_4^+, and N-NO_3^-) and DOC in treated soils during the incubation experiments are presented in Tables 3 and 4. The N_{tot} and N-NO_3^- levels gradually increased during incubation, regardless of the treatment, in luvisol, whereas the N-NO_3^- contents in fluvisol increased by one order of magnitude in the 1st week of

Table 2 Specific surface area and pore volume of the investigated biochars

	Biochar				
	300 °C	350 °C	400 °C	450 °C	500 °C
BET surface area ($m^2\ g^{-1}$)	0.83	0.84	16.48	179.82	385.65
t-plot surface area ($m^2\ g^{-1}$)	-	-	7.91	18.32	58.94
Total pore volume of pores less than 40.3122 nm diameter at p/p° = 0.950000000 ($cm^3\ g^{-1}$)	-	-	0.0081	0.0802	0.1826
t-plot micropore volume ($cm^3\ g^{-1}$)	-	-	0.0038	0.0686	0.1465
Micropore volume Dubinin-Astakhov ($cm^3\ g^{-1}$)			0.0076	0.0894	0.1791
Total intrusion volume (cm^3/g)	0.8176	0.8761	0.6850	1.0564	0.8176
Porosity (%)	52.82	53.38	48.27	58.00	52.82

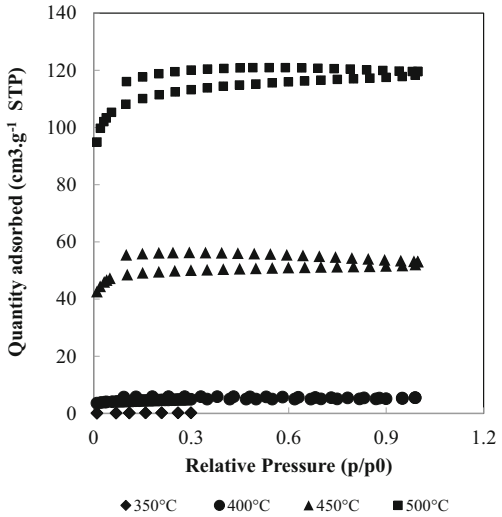

Fig. 1 N_2 adsorption and desorption isotherms of a woodchip biochar at different temperatures

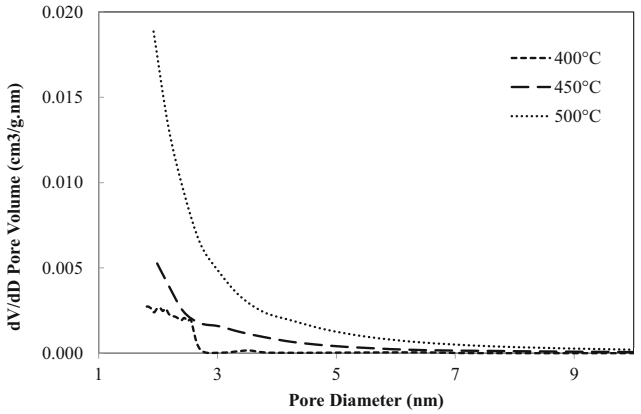

Fig. 3 Distribution of mesopore volume of woodchip biochar at different pyrolysis temperatures determined by using the BJH method

incubation, followed by doubling in the 2nd week, and remained relatively stable until the end of the experiment. A different pattern was recorded for N-NH_4^+, where a slight increase of the N-NH_4^+ contents was determined in the first 2 weeks, followed by a stepwise decrease until the end of the incubation in luvisol. In fluvisol, the N-NH_4^+ contents decreased after 1 week of incubation and remained relatively stable until the end of the experiment, suggesting the possible loss of the N-NH_4^+ in the sandy fluvisol during the incubation. Biochar application indicated trends (occasionally proven as significant at $p < 0.05$) to decrease the N_{tot} and N-NO_3^- contents in the treated soils with increasing pyrolysis temperatures. Regarding the N-NH_4^+ contents in luvisol, there was a significant decrease ($p < 0.05$) in the soil treated with biochar pyrolyzed at 500 °C, except for the 1st week of incubation. On the contrary, the N-NH_4^+ contents of the soils treated with biochars pyrolyzed at 300–350 °C tended to increase and/or remained unchanged compared to the control. In fluvisol, a significant ($p < 0.05$) decrease in N-NH_4^+ contents in the soil

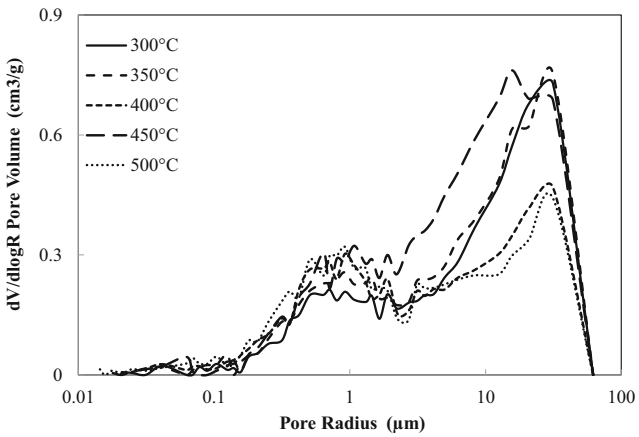

Fig. 2 Distribution of macropore volume of woodchip biochar at different pyrolysis temperatures determined by the mercury porosimetry

treated with biochar pyrolyzed at 500 °C was observed after the 3rd week of incubation; there were no changes in N-NH_4^+ contents in the soil treated with biochars pyrolyzed at temperatures between 300 and 400 °C compared to the control. Therefore, the potential adsorption of N-NH_4^+ on the applied biochar was affected more apparently by the biochar pyrolysis temperature than by the soil properties. As reviewed by Gul and Whalen (2016), the adsorption of N-NH_4^+ on wood-based biochar is responsible for the decrease in nitrification rates in the treated soils. In this context, Zhu et al. (2019) used biochar capping to reduce the N release from the sediments of a eutrophic lake. However, an increase in soil nitrification was observed with the additional application of an easily available N source (Gul and Whalen 2016; Gundale and DeLuca 2007). For instance, the application of swine manure mixed with biochar resulted in reduced gaseous N losses and increased yield and N uptake by *Brassica chinensis* (Zhang et al. 2019).

Regarding DOC, no changes were observed for luvisol, regardless of the soil treatment. In fluvisol, the DOC contents tended to increase in the soils treated with biochar pyrolyzed at 500 °C. This pattern confirms the stability of biochar-based carbon, at least within the duration of this experiment. Although the effect of biochar on the soil pH was not proven by this experiment, Pearson's correlation coefficients indicated the effects of pH on the mobile contents of inorganic N forms, where higher N-NO_3^- and N_{tot} contents were significantly ($p < 0.05$) related to higher pH levels (r values varying between 0.48 and 0.89 during incubation). A similar pattern was observed for DOC, where Pearson's correlation coefficients varied between $r = 0.42$ and 0.84 during the incubation. On the contrary, N-NH_4^+ was significantly ($p < 0.05$) positively related to soil pH only at the first day of incubation ($r = 0.51$); from the 7th day of incubation, these relationships were negative (r values varying between − 0.42 and − 0.91, significant at $p < 0.05$).

The potential bioavailability of nitrogen in the biochar-treated soils remains questionable (Biederman and Harpole

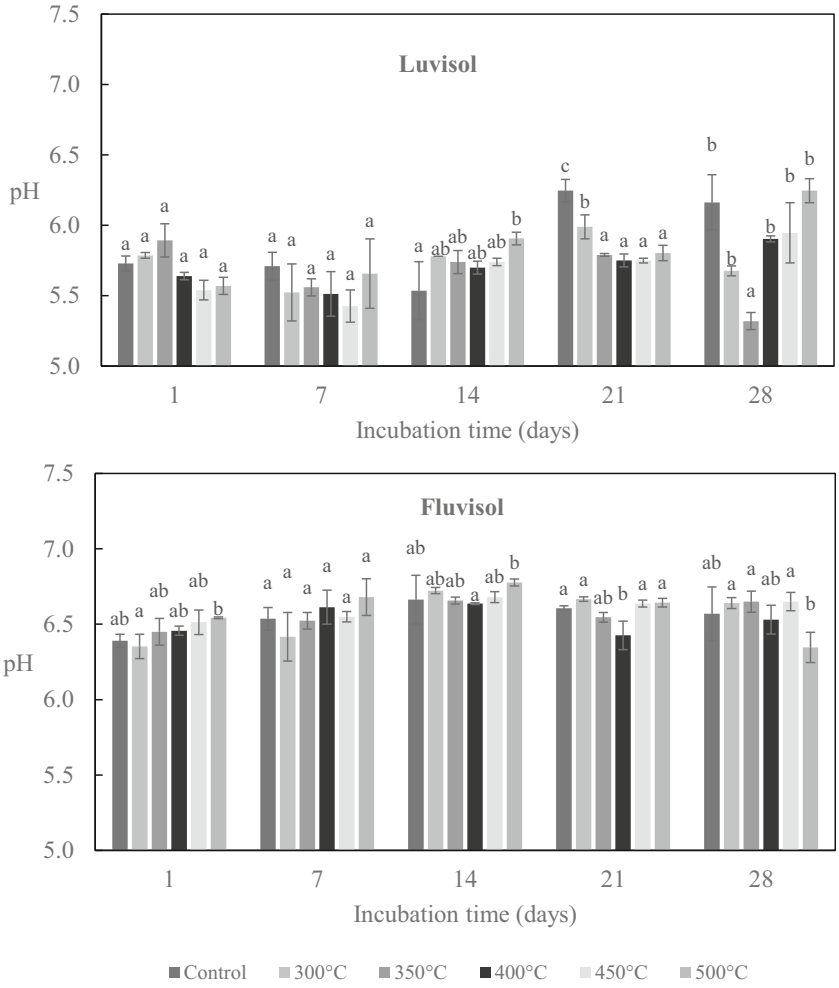

Fig. 4 The effect of biochar application on soil pH; the bars marked by the same letter did not significantly differ at $p < 0.05$ within individual sampling dates; data are presented as mean ± standard deviation, $n = 3$

2013). While Ca, P, and K can leach out from biochar under acidic conditions, nitrogen seems to be tightly incorporated into the biochar, making it unavailable for plants (Gaskin et al. 2008; Laird et al. 2010). These authors also identified heterocyclization of N during pyrolysis as the possible reason of the decreasing solubility of N. Nelissen et al. (2014) even reported a decreasing availability of nitrogen in the biochar-treated soil, resulting in decreased crop yields for these soils. In another study, the contents of available N (water-soluble) in giant reed (*Arundo donax*) biomass-based biochar decreased from 39 to 8 mg kg^{-1} with the increase of pyrolysis temperature from 350 to 600 °C (Zheng et al. 2013). However, the total N contents in wood-based biochars are generally low (Gul et al. 2015). In this experiment, there was no possibility to separate the potential effect of biochar on the availability of soil nitrogen and the mobility of the biochar-bound nitrogen.

Assessing the interrelationships among N_{tot}, N-NH_4^+, N-NO_3^-, and DOC (Supplementary Table S1), Pearson's correlation coefficients confirmed close positive correlations between N_{tot} and N-NO_3^- (r values varying between 0.55 and 0.99, significant at $p < 0.05$), where the weakest correlation was observed for the 1st day of incubation. The DOC levels correlated positively with both N_{tot} and N-NO_3^- (r values varying between 0.18 and 0.77, significant at $p < 0.05$). On the contrary, N-NH_4^+ contents were negatively correlated with N_{tot}, N-NO_3^-, and DOC levels (except for the 1st day of incubation), where r values varied between − 0.40 and − 0.83 (significant at $p < 0.05$). These relationships occurred regardless of the soil and/or biochar application. According to Gul et al. (2015), biochars produced at higher temperatures have more N-NO_3^-, while biochars produced at lower temperatures have a higher N-NH_4^+ proportion of the total N content. Decreasing N-NH_4^+ contents and, on the contrary, increasing N-NO_3^- contents in the soils treated with biochar (woody biochar pyrolyzed at 280 °C) were also published by Cordovil et al. (2019).

Sha et al. (2019) published a comprehensive meta-analysis of the potential volatilization of ammonia in biochar-treated soils, stating that wood-based biochars could be beneficial in the reduction of ammonia volatilization. In this study, the sorption behavior of N-NH_4^+ confirmed the differences among the biochars prepared at different pyrolysis temperatures, where no unambiguous sorption pattern was recorded for the biochars pyrolyzed at 300–350 °C, whereas both

Table 3 The contents of the mobile nitrogen species, DOC, MBC, and MBN in luvisol during the incubation experiment. The averages marked by the same letter did not significantly differ at $p < 0.05$ within individual columns; data are presented as mean ± standard deviation, $n = 3$

	N_{tot} (mg kg^{-1})	NO_3^- (mg kg^{-1})	NH_4^+ (mg kg^{-1})	DOC (mg kg^{-1})	MBC (mg C kg^{-1})	MBN (mg N kg^{-1})
Day 1						
Control	14.7 ± 1.5^{a}	2.15 ± 0.34^{a}	7.11 ± 0.48^{a}	73.8 ± 0.9^{a}	75.8 ± 9.0^{a}	8.39 ± 1.94^{ab}
300 °C	12.3 ± 0.6^{a}	1.95 ± 0.71^{a}	6.11 ± 1.00^{a}	74.8 ± 7.7^{a}	63.5 ± 6.6^{a}	11.3 ± 0.7^{b}
350 °C	14.1 ± 4.9^{a}	3.59 ± 2.60^{a}	5.48 ± 1.19^{a}	77.0 ± 2.1^{a}	56.5 ± 5.3^{a}	6.99 ± 3.59^{ab}
400 °C	14.7 ± 3.3^{a}	2.83 ± 1.49^{a}	7.48 ± 1.31^{a}	77.6 ± 4.8^{a}	63.9 ± 15.6^{a}	4.86 ± 1.74^{a}
450 °C	14.7 ± 2.5^{a}	2.49 ± 0.87^{a}	7.62 ± 0.66^{a}	83.1 ± 7.1^{a}	35.6 ± 10.7^{a}	2.35 ± 0.63^{a}
500 °C	13.7 ± 1.7^{a}	2.11 ± 0.38^{a}	6.37 ± 0.99^{a}	75.8 ± 8.2^{a}	61.1 ± 10.2^{a}	4.64 ± 0.91^{a}
Day 7						
Control	17.3 ± 0.7^{ab}	6.90 ± 0.97^{a}	7.79 ± 0.61^{a}	64.1 ± 0.5^{a}	18.4 ± 6.4^{a}	6.95 ± 0.82^{a}
300 °C	18.6 ± 3.5^{b}	7.91 ± 1.26^{a}	9.68 ± 1.47^{a}	64.3 ± 1.7^{a}	22.2 ± 2.5^{a}	4.76 ± 1.15^{a}
350 °C	18.2 ± 0.4^{ab}	6.86 ± 1.59^{a}	10.0 ± 1.1^{a}	65.6 ± 2.3^{a}	21.1 ± 4.6^{a}	6.74 ± 2.33^{a}
400 °C	14.4 ± 0.8^{a}	4.89 ± 1.27^{a}	7.23 ± 2.08^{a}	62.1 ± 1.2^{a}	17.8 ± 7.1^{a}	8.29 ± 1.74^{a}
450 °C	15.7 ± 2.2^{ab}	4.40 ± 1.00^{a}	7.83 ± 0.61^{a}	64.5 ± 4.7^{a}	15.4 ± 4.8^{a}	7.57 ± 1.09^{a}
500 °C	14.2 ± 2.4^{a}	4.48 ± 1.23^{a}	5.59 ± 2.61^{a}	63.9 ± 2.7^{a}	9.30 ± 0.60^{a}	6.00 ± 1.39^{a}
Day 14						
Control	30.1 ± 1.1^{a}	12.8 ± 2.0^{a}	12.9 ± 0.7^{b}	72.2 ± 2.1^{a}	13.0 ± 2.0^{a}	3.31 ± 0.31^{ab}
300 °C	27.0 ± 0.8^{a}	11.0 ± 0.8^{a}	10.6 ± 0.7^{b}	67.4 ± 2.2^{a}	19.8 ± 2.9^{a}	5.73 ± 0.93^{ab}
350 °C	23.8 ± 0.6^{a}	9.24 ± 1.42^{a}	12.1 ± 1.1^{b}	63.3 ± 0.0^{a}	20.6 ± 2.3^{a}	6.51 ± 1.09^{b}
400 °C	25.4 ± 2.9^{a}	11.4 ± 2.2^{a}	10.9 ± 0.6^{ab}	61.4 ± 0.4^{a}	20.5 ± 8.2^{a}	6.24 ± 0.81^{ab}
450 °C	23.7 ± 2.1^{a}	9.26 ± 0.97^{a}	11.1 ± 1.3^{ab}	63.0 ± 2.9^{a}	20.5 ± 0.5^{a}	4.11 ± 0.83^{ab}
500 °C	22.7 ± 4.2^{a}	8.42 ± 2.09^{a}	9.76 ± 0.66^{a}	68.3 ± 4.5^{a}	20.9 ± 5.1^{a}	1.79 ± 0.12^{a}
Day 21						
Control	33.5 ± 9.1^{a}	24.8 ± 4.0^{a}	6.12 ± 2.10^{ab}	76.5 ± 8.9^{a}	22.1 ± 3.6^{ab}	5.54 ± 1.39^{a}
300 °C	29.8 ± 1.6^{a}	21.6 ± 1.7^{a}	7.51 ± 2.07^{b}	67.7 ± 1.5^{a}	25.5 ± 3.6^{bc}	5.44 ± 1.70^{a}
350 °C	27.4 ± 2.0^{a}	18.7 ± 1.6^{a}	7.63 ± 0.68^{b}	68.2 ± 2.2^{a}	32.3 ± 4.4^{c}	5.10 ± 1.14^{a}
400 °C	29.2 ± 0.6^{a}	20.5 ± 0.8^{a}	5.94 ± 1.92^{ab}	71.3 ± 1.5^{a}	24.0 ± 5.7^{abc}	3.32 ± 0.51^{a}
450 °C	25.6 ± 2.6^{a}	17.1 ± 2.0^{a}	4.32 ± 1.45^{ab}	75.5 ± 1.1^{a}	20.0 ± 2.1^{ab}	6.51 ± 1.17^{a}
500 °C	21.1 ± 3.2^{a}	16.4 ± 2.9^{a}	2.33 ± 0.32^{a}	72.7 ± 2.8^{a}	13.4 ± 1.5^{a}	2.05 ± 0.71^{a}
Day 28						
Control	37.0 ± 5.1^{a}	26.9 ± 3.0^{a}	5.90 ± 0.92^{b}	83.5 ± 5.3^{a}	12.4 ± 3.5^{a}	20.8 ± 2.5^{a}
300 °C	32.9 ± 0.5^{a}	27.3 ± 1.5^{a}	4.01 ± 0.57^{ab}	80.6 ± 4.6^{a}	34.7 ± 3.2^{c}	17.2 ± 4.6^{a}
350 °C	32.2 ± 1.0^{a}	26.2 ± 1.2^{a}	4.10 ± 1.05^{ab}	78.8 ± 1.4^{a}	24.2 ± 4.7^{ab}	20.6 ± 4.1^{a}
400 °C	34.2 ± 0.4^{a}	26.5 ± 1.3^{a}	3.68 ± 0.79^{ab}	81.6 ± 2.8^{a}	21.2 ± 4.0^{ab}	20.9 ± 2.0^{a}
450 °C	29.3 ± 3.7^{a}	22.6 ± 3.5^{a}	3.60 ± 0.97^{ab}	83.0 ± 2.6^{a}	16.5 ± 3.5^{ab}	18.1 ± 2.5^{a}
500 °C	25.7 ± 0.9^{a}	19.4 ± 0.8^{a}	2.99 ± 0.98^{a}	79.5 ± 5.6^{a}	26.6 ± 1.6^{bc}	16.2 ± 0.9^{a}

Freundlich and Langmuir isotherms characterized the sorption pattern of the biochars prepared at ≥ 400 °C (Fig. 5). These results confirm the abovementioned biochar characteristics, namely that the temperature of 400 °C was the critical point splitting the biochars into two separate groups. The sorption behavior of the biochars described by the sorption isotherms was similar (Freundlich R^2 = 0.83, Langmuir R^2 = 0.93 for 400 °C biochar; Freundlich R^2 = 0.91, Langmuir R^2 = 0.98 for 450 °C biochar; Freundlich R^2 = 0.79, Langmuir R^2 = 0.91 for 500 °C biochar, respectively). Similarly, the maximum sorption characteristics of biochars as affected by the pyrolysis temperature were indicated by the maximum sorption capacity (Q_{max}) derived from the Langmuir equation, with Q_{max} = 13.3 mg g^{-1} for 400 °C biochar, Q_{max} = 14.8 mg g^{-1} for 450 °C biochar, and Q_{max} = 11.6 mg g^{-1} for 500 °C biochar, respectively. Fungo et al. (2019) showed reduced NH_3 and N_2O emissions from soil treated with biochar (woody biochar, pyrolyzed at 550 °C), where the effect persisted for at least 3 years. Thus, the effects of the biochar application should be investigated in long-term studies. The loss of N-NH_4^+ sorption at biochar produced with lower temperatures is linked to the low CEC of such biochars (Yuan et al. 2011) as well as to

Table 4 The contents of the mobile nitrogen species, DOC, MBC, and MBN in fluvisol during the incubation experiment. The averages marked by the same letter did not significantly differ at $p < 0.05$ within individual columns; data are presented as mean ± standard deviation, $n = 3$

	N_{tot} (mg kg^{-1})	NO_3^- (mg kg^{-1})	NH_4^+ (mg kg^{-1})	DOC (mg kg^{-1})	MBC (mg C kg^{-1})	MBN (mg N kg^{-1})
Day 1						
Control	21.6 ± 5.3^{a}	8.22 ± 1.51^{a}	9.68 ± 0.51^{a}	89.4 ± 2.2^{a}	26.2 ± 5.2^{a}	6.87 ± 1.59^{b}
300 °C	20.2 ± 0.2^{a}	6.99 ± 1.13^{a}	8.80 ± 0.37^{a}	84.6 ± 1.4^{a}	23.5 ± 8.6^{a}	1.41 ± 0.33^{a}
350 °C	40.4 ± 6.2^{a}	6.76 ± 1.89^{a}	9.37 ± 0.66^{a}	84.3 ± 3.1^{a}	30.3 ± 0.7^{a}	2.58 ± 0.54^{ab}
400 °C	27.5 ± 1.5^{a}	7.80 ± 1.27^{a}	8.23 ± 1.80^{a}	83.3 ± 1.2^{a}	28.3 ± 2.9^{a}	3.11 ± 0.59^{ab}
450 °C	22.1 ± 2.4^{a}	7.39 ± 1.33^{a}	6.60 ± 1.47^{a}	82.7 ± 4.2^{a}	32.2 ± 2.9^{a}	4.14 ± 0.44^{ab}
500 °C	26.5 ± 2.6^{a}	6.38 ± 2.16^{a}	12.2 ± 1.0^{a}	103 ± 9^{a}	23.2 ± 9.0^{a}	4.09 ± 1.00^{ab}
Day 7						
Control	43.9 ± 3.0^{a}	31.4 ± 5.5^{a}	2.65 ± 1.18^{a}	68.4 ± 6.7^{a}	21.1 ± 1.9^{c}	5.38 ± 0.73^{ab}
300 °C	41.0 ± 7.3^{a}	32.8 ± 7.1^{a}	2.70 ± 0.95^{a}	71.8 ± 4.5^{a}	18.0 ± 0.8^{bc}	9.86 ± 1.39^{b}
350 °C	35.2 ± 5.1^{a}	29.3 ± 4.8^{a}	1.39 ± 0.25^{a}	64.7 ± 3.0^{a}	6.74 ± 0.78^{a}	5.75 ± 0.21^{ab}
400 °C	44.8 ± 6.6^{a}	38.2 ± 8.1^{a}	1.63 ± 1.74^{a}	68.1 ± 0.5^{a}	10.9 ± 1.3^{ab}	2.30 ± 0.27^{ab}
450 °C	36.5 ± 3.4^{a}	29.1 ± 3.2^{a}	1.96 ± 0.91^{a}	70.2 ± 1.6^{a}	7.06 ± 1.78^{ab}	2.53 ± 0.18^{ab}
500 °C	28.9 ± 3.8^{a}	22.7 ± 2.2^{a}	1.69 ± 0.11^{a}	74.0 ± 6.3^{a}	13.9 ± 1.3^{b}	1.25 ± 0.19^{a}
Day 14						
Control	55.8 ± 2.9^{b}	44.5 ± 4.6^{b}	2.25 ± 0.21^{a}	80.5 ± 3.6^{ab}	41.8 ± 1.5^{c}	3.98 ± 0.36^{a}
300 °C	46.6 ± 1.2^{ab}	39.1 ± 3.0^{ab}	2.74 ± 1.74^{a}	78.2 ± 1.0^{a}	14.1 ± 3.5^{a}	7.08 ± 0.57^{a}
350 °C	48.3 ± 3.3^{ab}	41.0 ± 4.5^{b}	2.22 ± 1.58^{a}	78.4 ± 0.7^{ab}	18.4 ± 2.5^{ab}	9.96 ± 1.90^{a}
400 °C	45.5 ± 3.9^{ab}	39.5 ± 2.4^{b}	1.62 ± 1.24^{a}	83.6 ± 0.4^{ab}	22.5 ± 1.6^{b}	8.02 ± 2.47^{a}
450 °C	41.8 ± 3.0^{ab}	36.6 ± 2.6^{ab}	0.96 ± 0.46^{a}	78.5 ± 1.0^{ab}	19.2 ± 3.8^{ab}	6.81 ± 2.30^{a}
500 °C	36.8 ± 0.8^{a}	24.4 ± 5.5^{a}	2.59 ± 0.92^{a}	85.9 ± 7.4^{b}	21.8 ± 2.5^{ab}	3.45 ± 0.07^{a}
Day 21						
Control	56.6 ± 3.4^{a}	50.1 ± 4.5^{b}	3.79 ± 0.87^{b}	83.2 ± 7.7^{a}	37.6 ± 2.8^{b}	5.40 ± 0.32^{a}
300 °C	53.2 ± 4.6^{a}	46.5 ± 4.7^{ab}	2.34 ± 0.62^{ab}	79.9 ± 3.2^{a}	42.5 ± 3.5^{b}	9.71 ± 0.81^{ab}
350 °C	45.1 ± 3.2^{a}	38.3 ± 3.1^{ab}	3.02 ± 1.03^{ab}	77.9 ± 1.2^{a}	43.1 ± 8.4^{b}	23.5 ± 2.0^{c}
400 °C	50.6 ± 8.3^{a}	42.9 ± 6.5^{b}	3.03 ± 0.28^{ab}	80.8 ± 2.6^{a}	42.3 ± 3.0^{b}	9.09 ± 0.49^{ab}
450 °C	49.9 ± 4.4^{a}	39.5 ± 5.2^{ab}	3.21 ± 0.88^{ab}	88.3 ± 0.4^{a}	20.5 ± 1.5^{a}	8.38 ± 1.14^{ab}
500 °C	38.0 ± 8.5^{a}	26.6 ± 8.1^{a}	1.58 ± 0.50^{a}	88.5 ± 2.5^{a}	33.3 ± 4.3^{ab}	12.7 ± 2.6^{b}
Day 28						
Control	61.6 ± 0.7^{b}	52.3 ± 0.8^{b}	2.63 ± 0.12^{ab}	73.5 ± 6.0^{a}	39.3 ± 2.5^{a}	5.01 ± 0.84^{a}
300 °C	57.8 ± 0.2^{ab}	49.1 ± 0.5^{ab}	2.23 ± 0.47^{ab}	71.0 ± 1.5^{a}	29.2 ± 3.1^{a}	2.89 ± 0.69^{a}
350 °C	56.0 ± 2.6^{ab}	47.9 ± 2.1^{ab}	3.47 ± 0.95^{b}	71.7 ± 1.7^{a}	39.0 ± 5.3^{a}	6.71 ± 1.63^{ab}
400 °C	50.1 ± 3.2^{ab}	44.7 ± 2.5^{ab}	2.00 ± 0.38^{ab}	75.0 ± 0.0^{a}	27.2 ± 9.9^{a}	13.7 ± 0.9^{c}
450 °C	49.9 ± 2.0^{ab}	42.7 ± 2.5^{ab}	2.09 ± 1.03^{ab}	81.8 ± 8.1^{a}	29.1 ± 2.5^{a}	12.4 ± 1.9^{bc}
500 °C	39.9 ± 6.0^{a}	33.8 ± 5.7^{a}	1.36 ± 0.80^{a}	91.4 ± 2.9^{a}	38.8 ± 2.6^{a}	6.35 ± 0.99^{ab}

the lower surface area and pore size of undecomposed woody material (Fig. S2). The lower CEC of biochar produced at lower production temperatures (300 °C) and the increase toward 500 °C have been reported (Gai et al. 2014). Furthermore, the pyrolysis temperature clearly affected the N-NO_3^- sorption pattern of biochars, with no sorption of N-NO_3^- being observed for the biochars produced at a temperature of 450 °C and below and with maximum sorption of N-NO_3^-, up to 10.5 and 11.05 mg g^{-1}, for biochars produced at 500 and 450 °C, respectively, as estimated by the Langmuir equation (Fig. 6). The nitrate sorption capacity of biochars produced at lower temperatures could be again very low at temperatures below 450 °C, due to the low pore size and surface area of the undecomposed woody material (Yuan et al. 2011).

3.2.2 Microbial carbon and nitrogen biomass

Biochar preserves essential nutrients and moisture, facilitating microbial colonization in its periphery (Nanda et al.

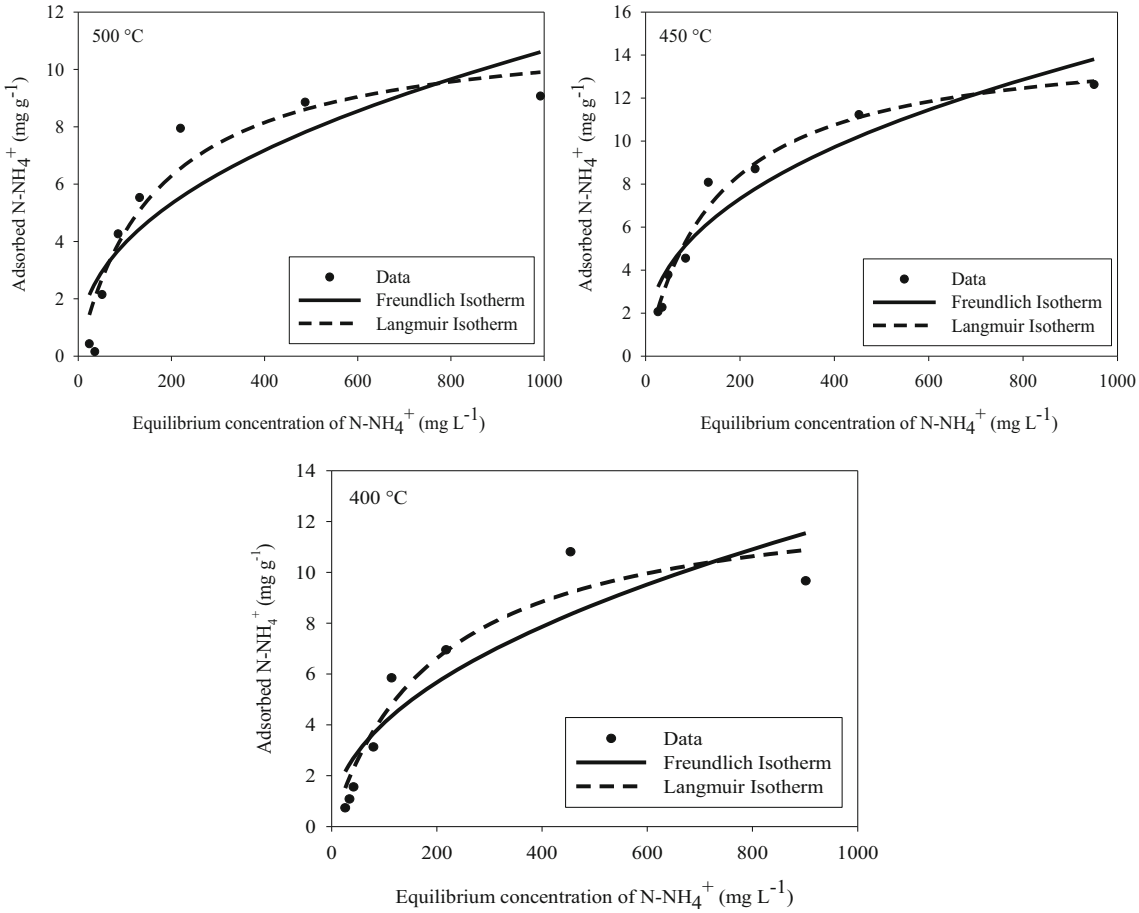

Fig. 5 The sorption pattern of $N\text{-}NH_4^+$ N on the biochars as affected by the pyrolysis temperature

2016). Ding et al. (2016) reviewed some mechanisms explaining how biochar affects microorganisms in soils: (i) changes in nutrient availability; (ii) changes in microbial communities; (iii) alterations in plant-microbe signaling. Thus, the alterations in the soil microbial communities can also affect soil fertility, resulting in changes in crop productivity. Cordovil et al. (2019) stated that the response of soil biological parameters to wood-based biochar differed according to the different experimental soils. These findings suggest that low decomposing microbial activity processes are directly promoted by biochar application. This experiment suggests a similar pattern (Tables 3 and 4), and the MBC levels differed according to the experimental soils. While the MBC levels in loamy luvisol strongly decreased, in sandy fluvisol, these values decreased in the 2nd week of cultivation and increased again until the end of the experiment. In both soils, the MBC levels responded differently to biochar application. In luvisol, the changes in MBC values started in the 3rd week of cultivation, where increasing MBC levels were recorded for the biochars produced at low temperatures (300 and 350 °C). On the contrary, decreasing MBC levels compared to the control were observed in fluvisol, even after 1 week of cultivation, and the levels were stable at the end of the experiment, regardless of the biochar applied.

A less apparent overall response to biochar application was observed for MBN (Tables 3 and 4). Based on the literature (for instance Tian et al. 2016), biochar application results in the increase of proteolytic enzymes (α-leucine aminopeptidases). These results indicate that the microorganisms are able to use nitrogen from soil organic matter to balance the shifted C/N ratio due to biochar application, therefore enhancing the cycling of the stabile nitrogen in soil (Tian et al. 2016). Similarly, Liao et al. (2016) reported enhanced activity of soil enzymes involved in N cycling after biochar application. In this experiment, the soil enzymatic activity was not measured, but the MBN levels correlated significantly with the $N\text{-}NO_3^-$ contents in the soils (r values varied between − 0.35 and − 0.54; significant at $p < 0.05$), supporting the possibility of improved N use in the biochar-treated soils (Supplementary Table S1). However, the effects of biochar application were ambiguous and did not show any clear trends, according neither to the biochar pyrolysis temperature nor to the duration of the incubation.

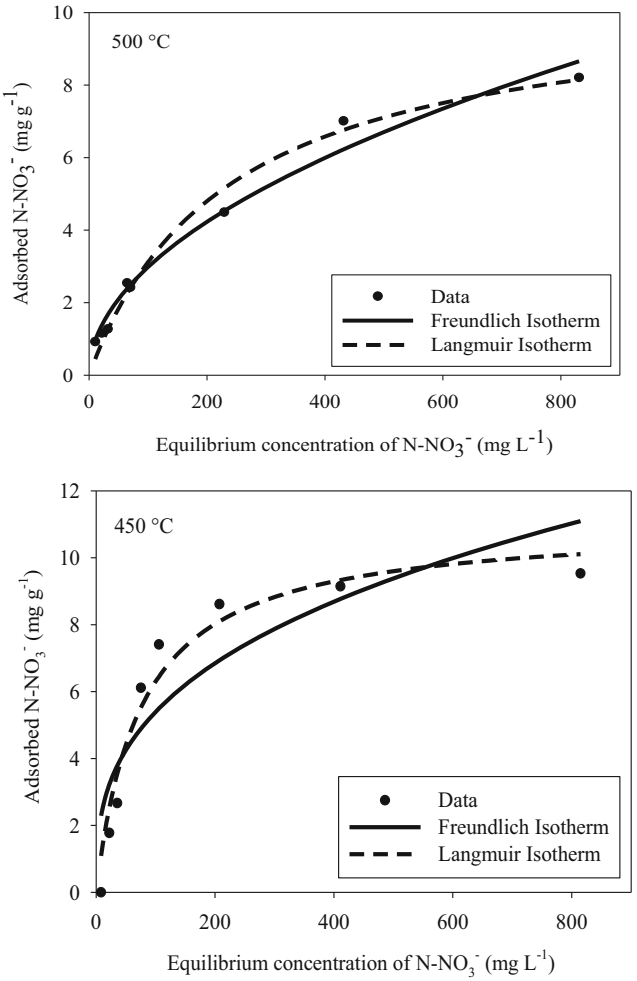

Fig. 6 The sorption pattern of $N\text{-}NO_3^-$ on the biochars as affected by the pyrolysis temperature

Ahmad et al. (2016) observed enhanced abundance of soil microorganisms in the soils treated by low-temperature biochar (300 °C) due to the increased proportion of DOM, whereas the abundance of the microorganisms in the soils treated by high-temperature (700 °C) biochars remained unchanged. In this experiment, however, the DOC levels remained unchanged in most of the biochar-treated variants compared to the control, and occasionally, the DOC levels even indicated the opposite trend (Table 3). Throughout the experiment, the MBC levels were moderately correlated with DOC, regardless of the sampling date and the pyrolysis temperature, where significant ($p < 0.05$) Pearson's correlation coefficients (r) reached 0.273 for luvisol and 0.278 for fluvisol (Supplementary Table S1). A comparison of both soils showed a substantial role of soil physicochemical parameters, especially the differences in the Cox contents in the experimental soils. Gul et al. (2015) showed that high-temperature biochars prepared from feedstocks with low-nutrient contents (such as woodchips) can result in the reduction of the growth of the microbial communities for 2–3 months after the application if applied to soil with a low organic matter content. Thus, the decrease of the MBC levels during incubation of luvisol (Fig. 3a) could be related to the low Cox content (0.93%) of this soil, whereas the MBC levels in fluvisol showed the opposite trend during incubation (Fig. 3b). Multivariate analysis of the data (Table 5) confirmed the significant effect of biochar application and incubation time on all measured variables. However, the mutual effect of biochar application and experimental soil was proven only occasionally, due to the contradictory effects of biochar application on the individual soils. Kuppusamy et al. (2016) concluded that long-term biochar amendment studies at field scale are required to study the following: (i) changes in the biochar surface chemistry and soil physical properties in all situations; (ii) essential, trace, and toxic element availability and movement in soil; and (iii) influence on the abundance or minimization of beneficial soil microbes as well as on weeds and crop growth. Yadav et al. (2019) reported increasing microbial activity and microbial biomass carbon

Table 5 Summary of 3-way ANOVA of the effects of soil, biochar, and incubation time on the mobile nitrogen species, DOC, MBC, MBN, and soil pH

	Incubation time	Soil	Biochar	Incubation time × soil	Incubation time × biochar	Soil × biochar	Incubation time × soil × biochar
pH	30.4***	3362***	7.17***	20.7***	6.28***	7.15***	9.78***
Total N	72.6***	425***	9.67***	3.58**	ns	ns	ns
Nitrate	419***	1445***	28.6***	58.5***	2.71***	7.96***	ns
Ammonia	65.4***	259***	4.53***	83.4***	2.15**	7.23***	2.78***
DOC	59.8***	125***	9.95***	22.5***	ns	6.85***	1.95*
MBC	81.7***	ns	6.20***	65.4***	3.19***	3.45**	4.40***
MBN	143***	31.4***	13.6***	130***	9.34***	5.68***	10.6***

Values shown represent *F*-value of 3-way ANOVA

ns not significant

*$p < 0.05$; **$p < 0.01$; ***$p < 0.001$

after application of aged biochar (produced from *Cymbopogon winterianus* biomass as feedstock) compared to fresh biochars.

4 Conclusions

Our results confirm the importance of the pyrolysis temperature, resulting in qualitatively different biochars varying in their morphological structure, physicochemical properties, and in the response to the biochar interaction with the soil structures and the soil microbiome. For this particular feedstock, i.e., woodchips, 400 °C seemed to be the critical point, indicating the substantial change in the characteristics of the biochar and with a substantial difference in the sorption behavior of N-NH_4^+ and N-NO_3^- below and above this temperature. The results of the biochar characterization documented that the material pyrolyzed at the temperatures lower than 400 °C does not belong to the typical biochars with the fully developed porous structure. The low contents of N in the biochars do not allow suggesting this material as a source of N; on the contrary, the application of such a material can reduce the mobile proportions of N-NH_4^+, indicating the positive role of woodchip-based biochar in the stabilization of the inorganic nitrogen forms in the soil.

In the case of biological parameters, given as MBC and MBN levels, the results indicate that these changes occur over a longer period than that in the current study. Long-term field trials need to be conducted to test whether soil properties can be influenced permanently through biochar application. In this sense, for soil functionality and biological activity assessments, the behavior of the soil microbiota in contact with biochar in the soil needs to be investigated, and the potential ability of these organisms to transform and/or decompose biochar in the soil should be elucidated in further research.

Supplementary Information The online version contains supplementary material available at https://doi.org/10.1007/s11368-021-02910-5.

Acknowledgements Correction and improvement of language were provided by Proof-Reading-Service.com Ltd., Devonshire Business Centre, Works Road, Letchworth Garden City SG6 1GJ, UK.

Funding The authors received financial support from the GAČR 19-02836S project, and European Regional Development Fund - Project No. CZ.02.1.01/0.0/0.0/16_019/ 0000845.

References

Ahmad M, Ok YS, Kim BY, Ahn JH, Lee YH, Zhang M, Moon DH, Al-Wabel MI, Lee SS (2016) Impact of soybean stover- and pine needle-derived biochars on Pb and As mobility, microbial community, and carbon stability in a contaminated agricultural soil. J Environ Manag 166:131–139

Azargohar R, Nanda S, Rao B, Dalai A (2013) Slow pyrolysis of deoiled canola meal: product yields and characterization. Energ Fuel 27: 5268–5279

Barrett EP, Joyer LG, Halenda PP (1951) The determination of pore volume and area distributions in porous substances I. Computations from nitrogen isotherms. J Am Chem Soc 73:373–380

Bates RB, Ghoniem AF (2012) Biomass torrefaction: modeling of volatile and solid product evolution kinetics. Biores Technol 124:460–469

Beesley L, Moreno-Jiménez E, Gomez-Eyles JL, Harris E, Robinson B, Sizmur T (2011) A review of biochars' potential role in the remediation, revegetation and restoration of contaminated soils. Environ Pollut 159:3269–3282

Bergman PCA, Kiel JHA (2005) Torrefaction for biomass upgrading. ECN report, ECN-RX—05-180

Biederman L, Harpole W (2013) Biochar and its effects on plant productivity and nutrient cycling: a meta-analysis. GCB Bioenergy 5:202–214

Břendová K, Száková J, Lhotka M, Krulikovská T, Punčochář M, Tlustoš P (2017) Biochar physicochemical parameters as a result of feedstock material and pyrolysis temperature: predictable for the fate of biochar in soil? Environ Geochem Health 39:1381–1395

Brewer CE, Chuang VJ, Masiello CA, Gonnermann H, Gao X, Dugan B, Driver LE, Panzacchi P, Zygourakis K, Davies CA (2014) New approaches to measuring biochar density and porosity. Biomass Bioenerg 66:176–185

Brookes PC, Landman A, Pruden G, Jenkinson DS (1985) Chloroform fumigation and the release of soil nitrogen: a rapid direct extraction method for measuring microbial biomass nitrogen in soil. Soil Biol Biochem 17:837–842

Brown J, Renvoize S, Chiang Y, Ibaragi Y, Flavell R, Greef J, Huang L, Hsu T, Kim D, Hastings A, Schwarz K, Stampfl P, Valentine J, Yamada T, Xi Q, Donnison I (2011) Developing Miscanthus for bioenergy. In: Karp A (ed) Halford NG. The Royal Society of Chemistry, Energy crops, pp 301–321

Brunauer S, Emmett PH, Teller E (1938) Adsorption of gases in multimolecular layers. J Am Chem Soc 60:309–319

Chen X, Chen G, Chen L, Chen Y, Lehmann J, McBride MB, Hay AG (2011) Adsorption of copper and zinc by biochars produced from pyrolysis of hardwood and corn straw in aqueous solution. Biores Technol 102:8877–8884

Chen BL, Zhou DD, Zhu LZ (2008) Transitional adsorption and partition of nonpolar and polar aromatic contaminants by biochars of pine needles with different pyrolytic temperatures. Environ Sci Technol 42:5137–5143

Ciulu M, Ollivier N, Demelas C, Boudenne JL, Coulomb B, Théraulaz F, Robert-Peillard F (2018) A highly-sensitive microplate fluorimetric method for the high-throughput determination of nitrate ion in aqueous compost extracts. Microchem J 138:424–429

Cordovil CMS, Pinto R, Silva B, Sas-Paszt L, Sakrabani R, Skiba UM (2019) The impact of woody biochar on microbial processes in conventionally and organically managed arable soils. Commun Soil Sci Plant Anal 50:1387–1402

Ding Y, Liu Y, Liu S, Li Z, Tan X, Huang X, Zeng G, Zhou L, Zheng B (2016) Biochar to improve soil fertility. Agron Sustain Dev 36:36

Dutta B, Raghavan VGS, Orsat V, Ngadi M (2015) Surface characterisation and classification of microwave pyrolysed maple wood biochar. Biosyst Eng 131:49–64

Fungo B, Lehmann J, Kalbitz K, Thionĝo M, Tenywa M, Okeyo I, Neufeldt H (2019) Ammonia and nitrous oxide emissions from a field ultisol amended with tithonia green manure, urea, and biochar. Biol Fertil Soils 55:135–148

Gai X, Wang H, Liu J, Zhai L, Liu S, Ren T, Liu H (2014) Effects of feedstock and pyrolysis temperature on biochar adsorption of ammonium and nitrate. PLoS ONE 9:1–9

García-Sánchez M, Klouza M, Holečková Z, Tlustoš P, Száková J (2016) Organic and inorganic amendment application on mercury-polluted soils: effects on soil chemical and biochemical properties. Environ Sci Pollut Res 23:14254–14268

Gaskin J, Steiner C, Harris K, Das K, Bibens B (2008) Effect of low-temperature pyrolysis conditions on biochar for agricultural use. Transact ASABE 5:2061–2069

Gregorich EG, Voroney RP, Kachanoski RG (1990) Calibration of rapid direct chloroform extraction method for measuring soil microbial biomass C. Soil Biol Biochem 22:1009–1011

Gul S, Whalen JK (2016) Biochemical cycling of nitrogen and phosphorus in biochar-amended soils. Soil Biol Biochem 103:1–15

Gul S, Whalen JK, Thomas BW, Sachdeva V, Deng H (2015) Physico-chemical properties and microbial responses in biochar-amended soils: mechanisms and future directions. Agric Ecosyst Environ 206:46–59

Gundale MJ, DeLuca TH (2007) Charcoal effects on soil solution chemistry and growth of *Koeleria macrantha* in the ponderosa pine/Douglas fir ecosystem. Biol Fertil Soils 43:303–311

Hailegnaw NS, Mercl F, Pračke K, Száková J, Tlustoš P (2019a) High temperature-produced biochar can be efficient in nitrate loss prevention and carbon sequestration. Geoderma 338:48–55

Hailegnaw NS, Mercl F, Pračke K, Száková J, Tlustoš P (2019b) Mutual relationships of biochar and soil pH, CEC, and exchangeable base cations in a model laboratory experiment. J Soils Sedim 19:2405–2416

IUPAC (2015) Physisorption of gases, with special reference to the evaluation of surface area and pore size distribution (IUPAC Technical Report). Tech Rep 87:1051–1069. https://doi.org/10.1515/pac-2014-1117

Jimenez-Cordero D, Heras F, Alonso-Morales N, Gilarranz MA, Rodriguez JJ (2013) Porous structure and morphology of granular chars from flash and conventional pyrolysis of grape seeds. Biomass Bioenerg 54:123–132

Kan T, Strezov V, Evans TJ (2016) Lignocellulosic biomass pyrolysis: a review of product properties and effects of pyrolysis parameters. Renew Sust Energ Rev 57:1126–1140

Kuppusamy S, Thavamani P, Megharaj M, Venkateswarlu K, Naidu R (2016) Agronomic and remedial benefits and risks of applying biochar to soil: current knowledge and future research directions. Environ Int 87:1–12

Laird D, Fleming P, Davis D, Horton R, Wang B, Karlenn D (2010) Biochar impact on nutrient leaching from a Midwestern agricultural soil. Geoderma 158:443–449

Lehmann J (2007) Bio-energy in the black. Front Ecol Environ 5:381–387

Lehmann J, Rillig MC, Thies J, Masiello CA, Hockaday WC, Crowley D (2011) Biochar effects on soil biota–a review. Soil Biol Biochem 43:1812–1836

Liao N, Li Q, Zhang W, Zhou GW, Ma LJ, Min W, Ye J, Hou ZN (2016) Effects of biochar on soil microbial community composition and activity in drip-irrigated desert soil. Eur J Soil Biol 72:2–34

Limousin G, Gaudet JP, Charlet L, Szenknect S, Barthes V, Krimissa M (2007) Sorption isotherms: a review on physical bases, modeling and measurement. Appl Geochem 22:249–275

Lu Q, Li W, Zhu X (2009) Overview of fuel properties of biomass fast pyrolysis oils. Energy Conv Manag 30:1479–1493

Melo L, Coscione A, Abreu C, Puga A, Camargo O (2013) Influence of pyrolysis temperature on cadmium and zinc sorption capacity of sugar cane straw–derived biochar. BioResources, North America, 8, Aug. 2013. Available at: <http://ojs.cnr.ncsu.edu/ index.php/BioRes/article/view/BioRes_08_4_Melo_Pyrolysis_Cadmium_Zinc_Sorption>.

Mingorance MD, Barahona E, Fernandez-Galvez J (2007) Guidelines for improving organic carbon recovery by the wet oxidation method. Chemosphere 68:409–413

Mohanty P, Nanda S, Pant K, Naik S, Kozinski J, Dalai A (2013) Evaluation of the pyrolysis of the physicochemical development of biochars obtained from pyrolysis of wheat straw, Timothy grass and pinewood: effects of heating rate. J Anal Appl Pyrol 104:485–493

Nanda S, Azargohar R, Kozinski J, Dalai J (2014) Characteristic studies on the pyrolysis products from hydrolyzed Canadian lignocellulosic feedstock. Bioenerg Res 7:174–191

Nanda S, Dalai A, Berruti F, Kozinski J (2016) Biochar as an exceptional bioresource for energy, agronomy, carbon sequestration, activated carbon and speciality materials. Waste Biomass Valor 7:201–235

Nelissen V, Saha B, Ruysschaert G, Boeckx P (2014) Effect of different biochar and fertilizer types on N2O and NO emissions. Soil Biol Biochem 70:244–255

Novak J, Lima I, Xing B, Gaskin J, Steiner C, Das K, Schomberg H (2009) Characterization of designer biochar produced at different temperatures and their effects on a loamy sand. Ann Environ Sci 3:195–206

Novotny EH, Branco de Freitas Maia CM, de Melo Carvalho MT, Madari BE (2015) Biochar: pyrogenic carbon for agricultural use-a critical review. R Bras Ci Solo 39:321–344

Rafiq MK, Bachmann RT, Rafiq MT, Shang Z, Joseph S, Long R (2016) Influence of pyrolysis temperature on physico-chemical properties of corn stover (*Zea mays* L.) biochar and feasibility for carbon capture and energy balance. PLoS ONE 11:e0156894

Robert-Peillard F, Barco EP, Ciulu M, Demelas C, Théraulaz F, Boudenne JL, Coulomb B (2017) High throughput determination of ammonium and primary amine compounds in environmental and food samples. Microchem J 133:216–221

Sasidharan S, Torkzaban S, Bradford SA, Kookana R, Page D, Cook PG (2016) Transport and retention of bacteria and viruses in biochar-amended sand. Sci Total Environ 548-549:100–109

Sedláková M, Száková J, Tlustoš P (2019) The accessibility of biochar-bearing nutrients in soil as affected by the pyrolysis conditions. In: Proc. 15th International Conference on the Biogeochemistry of Trace Elements (ICOBTE 2019) in Nanjing, p. S-2-P5.

Sha Z, Li Q, Lv T, Misselbrook T, Liu X (2019) Response of ammonia volatilization to biochar addition: a meta-analysis. Sci Total Environ 655:1387–1396

Stefanidis S, Kalogiannis K, Iliopoulou E, Michailof C, Pilavachi P, Lappas A (2014) A study of lignocellulosic biomass pyrolysis via the pyrolysis of cellulose, hemicelluloses and lignin. J Anal Appl Pyrol 105:143–150

Sun F, Li S (2014) Biochars improve aggregate stability, water retention, and pore-space properties of clayey soil. J Plant Nutr Soil Sci 177:26–33

Tian J, Wang J, Dippold M, Gao Y, Blagodatskaya E, Kuzyakov Y (2016) Biochar affects soil organic matter cycling and microbial functions but does not alter microbial community structure in a paddy soil. Sci Total Environ 556:89–97

Tripathi M, Sahu JN, Ganesan P (2016) Effect of process parameters on production of biochar from biomass waste through pyrolysis: a review. Renew Sust Energy Rev 55:467–481

Tůmová K, Száková J, Najmanová J, Tlustoš P (2020) Scrap metal deposits as potential sources of enhanced risk in soil and vegetation. Polish J Environ Stud 29:841–852

Warnock DD, Lehmann J, Kuyper TW, Rillig MC (2007) Mycorrhizal responses to biochar in soil–concepts and mechanisms. Plant Soil 300:9–20

Webb PA, Orr C (1997) Analytical methods in fine particle technology. Norcross, GA: Micromeritics Instrument Corporation.

Wu J, Joergensen R, Pommerening B, Chaussod R, Brookes P (1990) Measurement of soil microbial biomass C by fumigation-extraction-an automated procedure. Soil Biol Biochem 22:1167–1169

Wu W, Yang M, Feng Q, McGrouther K, Wang H, Lu H, Chen Y (2012) Chemical characterization of rice straw-derived biochar for soil amendment. Biomass Bioenerg 47:268–276

Yadav V, Jain S, Mishra P, Khare P, Shukla AK, Karak T, Singh AK (2019) Amelioration in nutrient mineralization and microbial activities of sandy loam soil by short term field aged biochar. Appl Soil Ecol 138:144–155

Yuan JH, Xu RK, Zhang H (2011) The forms of alkalis in the biochar produced from crop residues at different temperatures. Biores Technol 102:3488–3497

Zackrisson O, Nilsson MC, Wardle DA (1996) Key ecological function of charcoal from wildfire in the boreal forest. Oikos 77:10–19

Zhang X, Chen C, Chen X, Tao P, Jin Z, Han Z (2018) Persistent effects of biochar on soil organic carbon mineralization and resistant carbon pool in upland red soil, China. Environ Earth Sci 77:177

Zhang H, Voroney R, Price G (2015) Effects of temperature and processing conditions on biochar chemical properties and their influence on soil C and N transformations. Soil Biol Biochem 83:19–28

Zhang J, Zhuang M, Shan N, Zhao Q, Li H, Wang L (2019) Substituting organic manure for compound fertilizer increases yield and decreases NH_3 and N_2O emissions in an intensive vegetable production systems. Sci Total Environ 670:1184–1189

Zhao L, Cao X, Mašek O, Zimmerman A (2013) Heterogeneity of biochar properties as a function of feedstock sources and production temperatures. J Hazard Mat 256–257:1–9

Zheng H, Wang Z, Deng X, Zhao J, Luo Y, Novak J, Herbert S, Baoshan X (2013) Characteristics and nutrient values of biochars produced from giant reed at different temperatures. Biores Technol 130:463–471

Zhu Y, Tang W, Jin X, Shan B (2019) Using biochar capping to reduce nitrogen release from sediments in eutrophic lakes. Sci Total Environ 646:93–104